*Short Note*

# A Study of Ambient Noise over an Onshore Oil Field in Abu Dhabi, United Arab Emirates

by Mohammed Y. Ali, Karl A. Berteussen, James Small,[*] and Braham Barkat

Abstract   The characteristics of ambient noise over an onshore oil field in Abu Dhabi, United Arab Emirates, have been investigated using arrays of three-component broadband seismometers by means of spectral amplitude and array wavenumber analysis within a frequency range of 0.1–10 Hz. The experiment was conducted to better understand the characteristics and origins of microseism (0.15–0.4 Hz) and microtremor (about 2.0–3.0 Hz) signals that have been reported as being a hydrocarbon indicator above several reservoirs in the region. The results of this study indicate that the long-period double-frequency peaks of microseism signals are generated by oceanic storms in the Arabian Sea as confirmed by data acquired throughout the impact of Cyclone Gonu on the coast of Oman. The study demonstrates that a narrowband of microtremor signals has no clear correlation with the recorded microseism signals. Cyclical daily and weekly variations in the spectral amplitudes of the signals clearly correlate with human activity. The results of this study, therefore, indicate that in this location the microseism and microtremor signals are not related to the presence of hydrocarbons in the subsurface but may be attributed to meteorological and anthropogenic effects, respectively.

## Introduction

The ambient noise of the Earth has been extensively studied over the past couple of decades (e.g., Peterson, 1993; Kedar and Webb, 2005; Webb, 2007). At low frequency, the natural activity of ocean waves is dominated by microseisms that can be found at two distinct frequency bands. The first frequency band (primary microseisms) corresponds to the predominant ocean wave frequency, typically between 0.05 and 0.1 Hz (Oliver and Ewing, 1957; Gerstoft and Tanimoto, 2007). The secondary microseisms propagate at twice the frequency of ocean waves and are thus termed double frequency, usually between 0.1 and 0.2 Hz (Longuet-Higgins, 1950; Bromirski and Duennebier, 2002). Double-frequency microseisms have much higher spectral amplitudes than primary microseisms with peaks occurring around 0.2 Hz. These signals are most likely due to nonlinear interactions of ocean waves (Longuet-Higgins, 1950; Tanimoto, 2007; Webb, 2007). The level of double-frequency microseisms depends upon the amplitude of the interacting ocean waves, wind speed, the size and duration of the area of interaction, and the propagation characteristics of the wave field (Longuet-Higgins, 1950; Bromirski and Duennebier, 2002). Microseisms are thought to propagate predominantly as

fundamental-mode Rayleigh waves that do not attenuate rapidly (Haubrich and McCamy, 1969; Barstow *et al.*, 1989; Bromirski and Duennebier, 2002; Bonnefoy-Claudet *et al.*, 2006). As a result, double-frequency microseisms are observed at continental sites far removed from coastlines.

At higher frequency ($> 1$ Hz), the ambient seismic noise field is dominated by cultural and wind-generated noise, with wind being the predominant high-frequency noise source at remote sites (Withers *et al.*, 1996; McNamara and Buland, 2004). However, in urban locations human activities (e.g., traffic and factories) have been noted as the major source of noise displaying daily and weekly cyclical variations (Bonnefoy-Claudet *et al.*, 2006; Marzorati and Bindi, 2006).

In recent years a narrowband of microtremor signals of approximately 2–6 Hz, with a peak of around 3 Hz has been observed and reported over a number of hydrocarbon reservoirs predominantly in the Middle East, including several in Abu Dhabi. Many of these studies have been conducted by an industry–university consortium (Dangel *et al.*, 2003; Holzner *et al.*, 2005; Lambert *et al.*, 2009; Saenger *et al.*, 2009). Some of these studies (Dangel *et al.*, 2003) have suggested that a strong correlation exists between the occurrence of spectral anomalies in the microtremor range and the presence of hydrocarbons. Observations in these studies suggest

---

*Now at Managing Consultant, Mollegata 90, 4008 Stavanger, Norway.

that the microtremor signal is strongest directly over the hydrocarbon reservoir but diminishes toward the rim and is totally absent above nonreservoir locations. Related studies have suggested that microtremor data can also be useful in many other situations including reconnaissance exploration of frontier areas, monitoring of hydrocarbon reservoirs, structural imaging to reduce drilling risk, and assisting with well positioning (Holzner *et al.*, 2005; Saenger *et al.*, 2009). These studies have even suggested that a linear relationship exists between the observed microtremor signal and the total thickness of hydrocarbon-bearing layers (Dangel *et al.*, 2003; Holzner *et al.*, 2005; Walker, 2008).

Thus, there has been considerable interest and speculation in recent years as to the nature of microtremor signals observed over a number of hydrocarbon reservoirs around the world. Although the actual causes of this phenomenon are not well understood, it has been suggested that these signals are the result of resonance amplification or resonance scattering by hydrocarbons present in subsurface reservoirs (Dangel *et al.*, 2003; Holzner *et al.*, 2005; Walker, 2008; Holzner *et al.*, 2009). These theories assume that the driving force of the microtremor signal is the Earth's natural ambient vibration caused by ocean waves (i.e., double-frequency microseism signal) coupled with the nonlinear behavior of liquid hydrocarbons, water, and pore-rock materials interacting in the reservoirs to distort the microseism. Recently, Steiner *et al.* (2008) have applied time reverse modeling to suggest that the hydrocarbon reservoir zone itself is the origin of the low-frequency microtremor spectral anomalies by assuming that the microtremor signals are a result of microseism events.

In this article, the results of an ambient noise analysis performed on signals recorded over an onshore oil field in Abu Dhabi are presented. The purpose of this analysis is to investigate the source of the microseism and microtremor signals. The occurrence of a major cyclone during the acquisition of the survey provided the ideal situation in which to study the relationship between microseism and microtremor signals. Results from the survey indicate that for this area the ocean-generated microseism signals are not the source for these microtremor signals as claimed.

## Study Area and Data Acquisition

The experiment was carried out between 21 May and 17 June 2007 over a producing oil field in Abu Dhabi, United Arab Emirates (UAE) (Fig. 1a). During the acquisition of the data, a powerful tropical cyclone (Cyclone Gonu), the strongest recorded tropical cyclone in the Arabian Sea (le Comte, 2008) struck the coast of Oman (Fig. 2). Cyclone Gonu had developed in the eastern Arabian Sea on 1 June 2007, attaining peak wind speeds of 240 km/hr on 3 June before reaching the eastern coast of Oman on 5 June with wind speeds of 150 km/hr. It subsequently turned northward into the Gulf of Oman and dispersed after moving ashore along southern Iran on 7 June 2007. Continuous recording over a period of

27 days allowed the temporal response of Cyclone Gonu to be correlated with observed microseism activity.

The experiment included the deployment of 11 arrays (7 arrays centered at location A and 4 arrays centered at location B, Fig. 1b) of varying aperture sizes (30–3600 m). Each array consisted of five broadband stations with typical recording periods of 24 hrs. Location A was situated over the maximum oil column ($> 35$ m) of the reservoir, whereas location B was positioned over an area that was believed to contain insignificant quantities of oil. Two seismometers were placed at locations A and B and recorded continually throughout the entire survey.

The wave-field signals were recorded using six ultra sensitive three-component broadband seismometers (Guralp CMG-6TD) with a frequency response from 0.03 to 100 Hz, a sensitivity of 2000 V/m/sec, and a sampling rate of 200 Hz. All of the stations used Global Positioning System receivers for time synchronization. The seismometers were placed on concrete slabs in pits approximately 50 cm deep and oriented to the geographic north. The sensors were covered and buried for firm ground contact and wind shielding.

Various signal analysis techniques were applied to the data including time series and power spectral density analyses. Excessively noisy sections of signals (e.g., due to earthquakes) were removed. The data were split into 1 hr time series that were subdivided into 60 subwindows of 60 sec each, then transformed into the Fourier domain. The spectral estimates were averaged to reduce variance and were corrected for instrument response. A 5% cosine taper was applied to the data to reduce spectral leakage. Fourier amplitude spectra were analyzed both without smoothing and with the smoothing procedure of Konno and Ohmachi (1998) using a *b*-value of 40. The mean was removed from the data before stacking.

## Characteristics of Observed Ambient Noises

Figure 3 illustrates the spectral amplitudes of signals recorded at locations A and B. The figure shows that the ambient noise levels observed within the study area generally fall into three distinct frequency bands: microseism (0.1–1 Hz), microtremor (2–3 Hz), and time-varying high-frequency ($> 3$ Hz) noise. The following two sections detail the spectral amplitudes observed in the microseism and microtremor bands.

### Double-Frequency Microseism

Figure 3 shows that in the frequency range of 0.15–0.4 Hz, the noise spectrum is dominated by a strong and easily recognizable peak at around 0.2 Hz called the double-frequency microseism peak (Longuet-Higgins, 1950; Bromirski and Duennebier, 2002). It is believed that these microseism events occur as a result of a nonlinear interaction between two opposing ocean swells (Longuet-Higgins, 1950; Kedar and Webb, 2005; Tanimoto, 2007). Conditions that
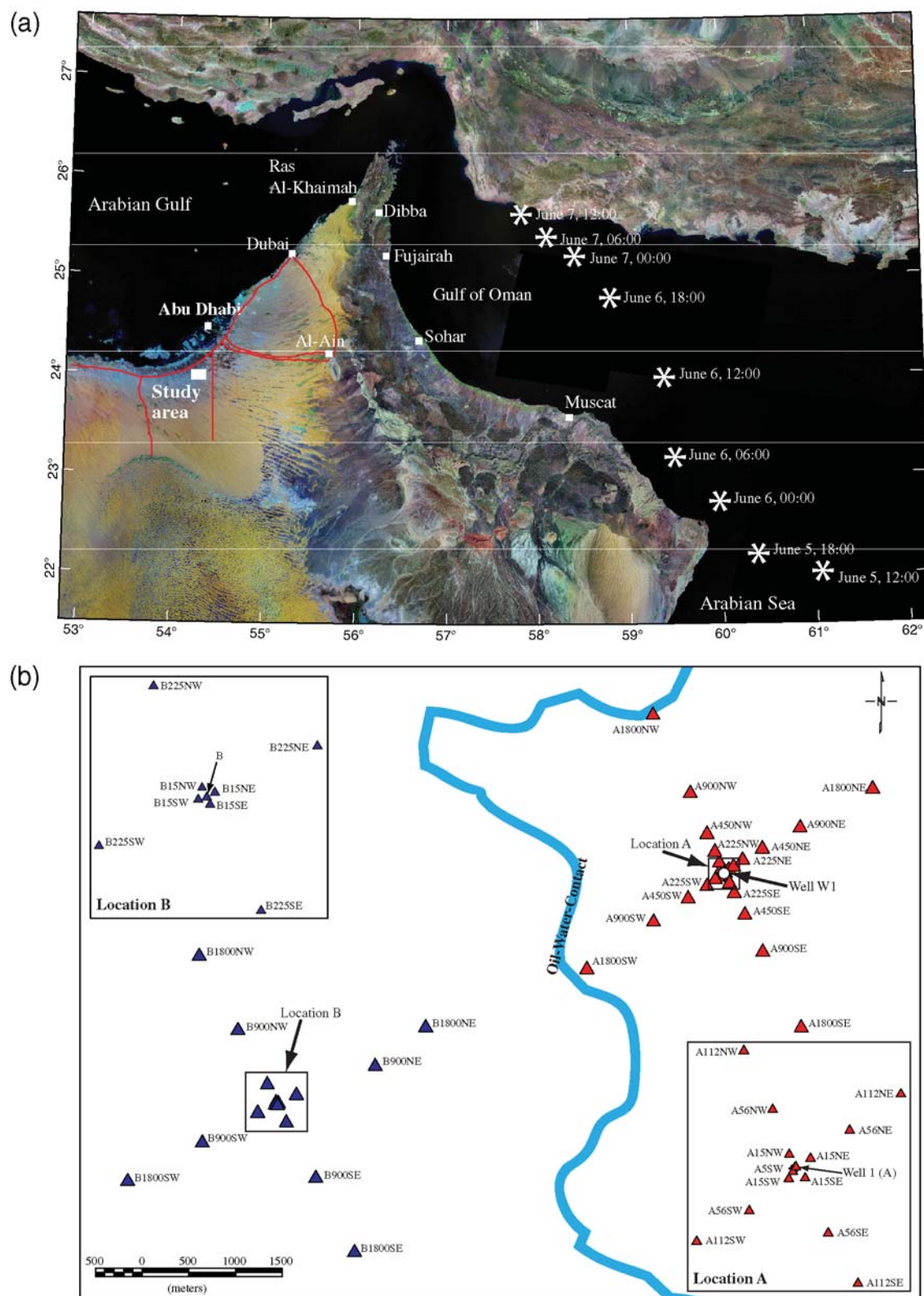
**Figure 1.**    (a) Regional satellite map showing the study area. Stars show the storm location. Red lines show major motorways. (b) Location map of the experiment showing the oil-water contact (OWC) of the oil field (blue line) superimposed over the recording stations. The sensor arrays consisted of six broadband instruments each deployed with varying aperture sizes. The oil field was selected as a suitable site for the experiment because it has a clear and well-defined OWC mapped from 3D seismic and well data.
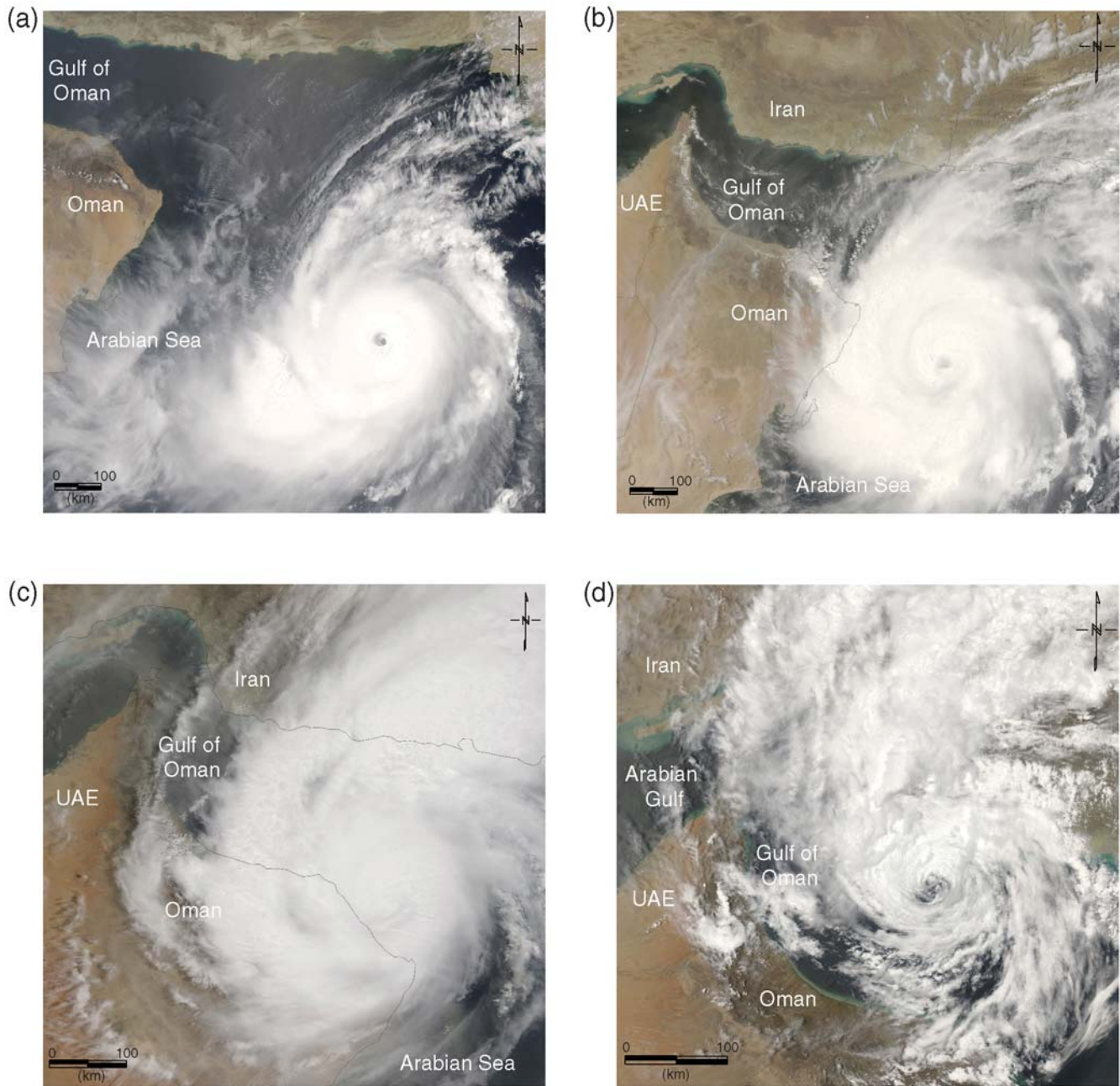
**Figure 2.** Satellite images of Oman and surrounding areas showing Cyclone Gonu striking the eastern coast of Oman (courtesy of National Aeronautics and Space Administration [NASA]). At 12:00 (local time) on 4 June 2007, Cyclone Gonu reached category 4 status with wind speeds over 240 km/hr. The images show a well-defined circular eye surrounded by dense clouds. (b) 09:35 on 5 June 2007, Cyclone Gonu was approaching the northeastern shore of Oman. (c) 10:15 on 6 June 2007, Cyclone Gonu was battering the Omani coast. (d) 12:55 on 7 June 2007, Cyclone Gonu had lost considerable power and was crossing the Gulf of Oman towards the Iranian coast.

could generate such a nonlinear interaction of antipodal sets of propagating waves may occur inside the center of a cyclonic depression. Alternatively, the interference of reflected waves arriving from all directions due to the incident swell and reflected/scattered wave energy from a nearby coastline could also be a contributing factor (Bromirski and Duennebier, 2002; Kedar and Webb, 2005; Gerstoft *et al.*, 2006).

We noted in this study that on some occasions the double-frequency peak split into two individual peaks, as is seen in the spectrum of the array data centered at location A acquired at midday on 4 June 2007 (Fig. 3c). The spectrum indicates two distinct double-frequency microseism peaks (a weaker peak at around 0.2 Hz and stronger peak at around 0.35 Hz) both linked with ocean activity. However, the spectral amplitudes of the data acquired on midday 7 June 2007 at locations A and B (Fig. 3a,b) indicate only one prominent double-frequency microseism peak at around 0.2 Hz. This type of double-frequency splitting has previously been
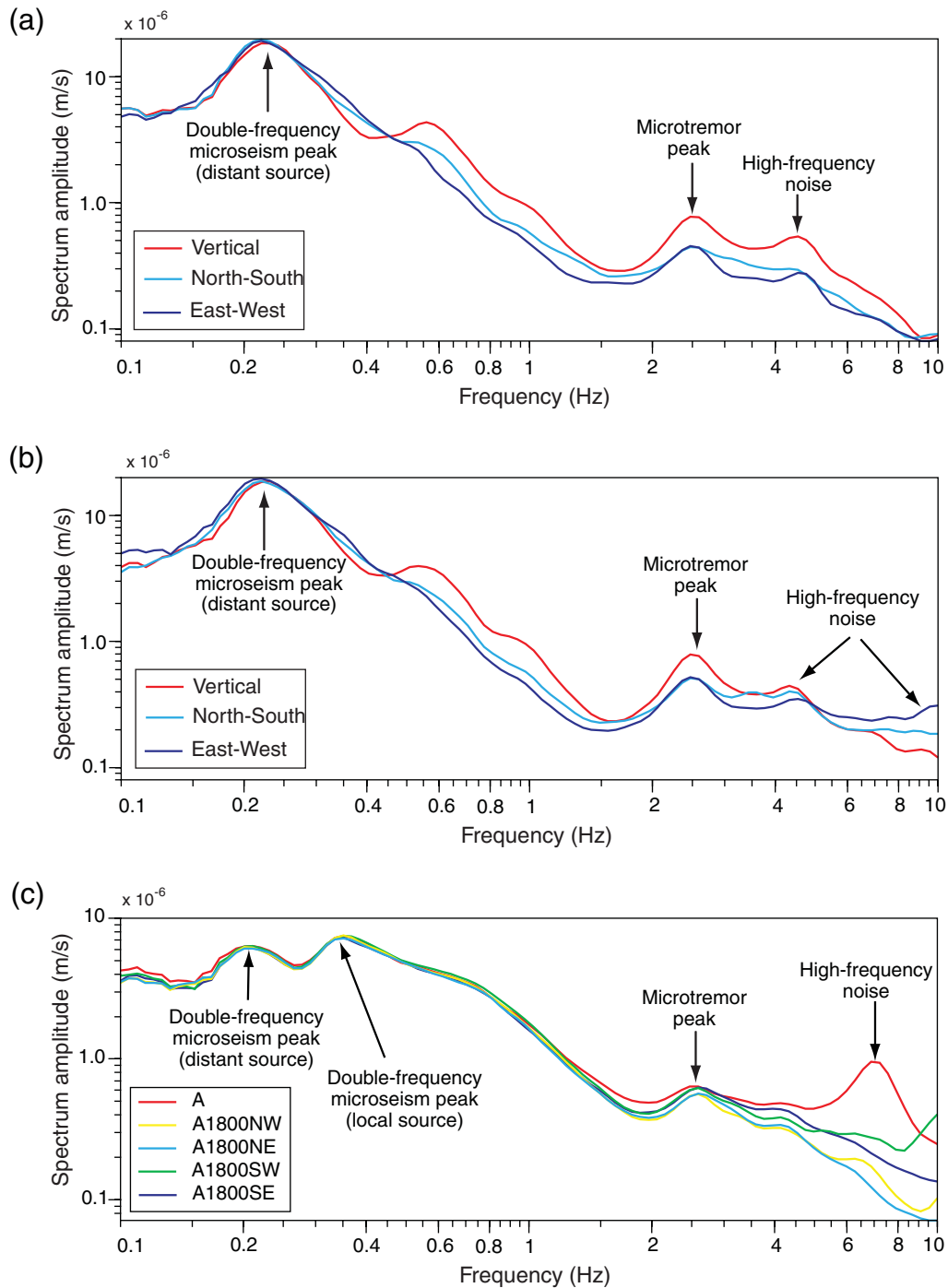
**Figure 3.** Examples of typical spectral amplitudes of vertical and horizontal components recorded at locations (a) A and (b) B on 7 June 2007 showing double-frequency microseism at a frequency of around 0.2 Hz, microtremor at a frequency of around 2.5 Hz, and high-frequency noise. Microseism and microtremor signals were observed on all three seismometer components (vertical, north–south, and east–west) at all recording stations. (c) Spectrum amplitude of a signal recorded on 4 June 2007 from array centered at location A with an aperture of 3600 m. Individual parts of the spectrum include long-period double-frequency microseism, short-period double-frequency microseism, microtremor signal, and high-frequency noise. The spectral amplitudes on the vertical and horizontal components are essentially identical. For sensor locations see Figure 1b.

reported in other studies (Bromirski *et al.*, 2005; Marzorati and Bindi, 2006), with reference to such peaks as being long-period double-frequency and short-period double-frequency microseisms. Findings in these studies concluded that short-

period double-frequency microseisms are generated by the rapid shift of local winds and nearby storms, whereas long-period double-frequency microseisms are often generated in near-coastal areas where the swells from distant

storms are reflected from the shoreline (Bromirski and Duennebier, 2002).

The correlation between the double-frequency microseism and the presence of ocean storms is supported by clear temporal associations between spectral amplitudes of long-period double-frequency microseisms observed during the approach of Cyclone Gonu and patterns of ocean swell obtained from satellite images. Figure 4a shows that the spectral amplitudes of long-period double-frequency microseism (center frequency of about 0.2 Hz) increased after 4 June 2007 when Cyclone Gonu approached the coast of Oman. The spectral amplitudes reached a maximum at approximately 01:00 on 6 June 2007, then dropped off but returned on 8 June to amplitudes similar to those before 4 June 2007 as the cyclone passed through the region. The increased spectral amplitudes recorded are consistent with increased intensity and proximity of the cyclone to the eastern Omani coast, which caused the superposition of ocean waves with waves reflected from shorelines as can be seen in the satellite images in Figure 2.

### Microtremor

Figure 3 presents a distinct spectral anomaly, referred to as microtremor, in the frequency band of around 2–3 Hz. All three components (vertical, north–south, and east–west) at all recording stations, whether positioned above the oil reservoir (location A) or outside the oil reservoir (location B) recorded this microtremor signal. In other studies, these signals have been interpreted as being related to nonlinear interactions of microseism signals within hydrocarbon reservoirs (Holzner *et al.*, 2005; Walker, 2008).

Figure 4b,c shows the time-variable characteristics of the spectral amplitudes in the microtremor band recorded on the vertical component at location B. The microtremor signal clearly exhibits cyclical variations (daily and weekly) in spectral amplitude with the minimum occurring between 01:00 and 03:00 (local time) and the maximum around 08:00. A general decrease in spectral amplitude is observed on weekends compared with weekdays. While the amplitudes observed on Fridays (the weekend in the UAE) are lower than those on other days, daily variations can still be clearly identified. More detailed analysis (Fig. 4c) shows that the spectral amplitude increases dramatically at around 08:00 (when trucks are permitted to enter nearby Abu Dhabi city) and decreases at 13:00 (prayer and lunch break for truck drivers) then increases again (during the afternoon rush hour) before falling to a minimum spectral amplitude at 01:00. These observations indicate that the source of the microtremors in the frequency around 2.5 Hz are clearly related to human activities, such as traffic noise, which reduce during the night and on weekends. Such daily and weekly cyclical variations of microtremor amplitudes have been reported in other studies (Yamanaka *et al.*, 1993; Bonnefoy-Claudet *et al.*, 2006). For example, in a study carried out on an oil field in Libya, Hanssen and Bussat (2008) correlated

the microtremor signal with surface waves caused by anthropogenic noises (e.g., production facilities, traffic), resonance frequency of the unconsolidated material in the area, and local topography (height of sand dunes). Moreover, it is well established that coupling of the noise generated from local cultural activity (e.g., traffic, production installations) and weather conditions (e.g., wind effects) dominates the noise at frequencies above 1.0 Hz (Withers *et al.*, 1996; McNamara and Buland, 2004; Marzorati and Bindi, 2006).

During the period that Cyclone Gonu was battering the Omani coast, the microseism signal increased significantly by a factor of around 10, whereas the microtremor signal remained seemingly unchanged, displaying only diurnal variations. These fundamental observations are contrary to the assumptions of other studies that have suggested that the driving force of the microtremor signals are microseism events (Holzner *et al.*, 2005, 2009). Such studies have typically not performed detailed analyses of ambient noise over long time periods; hence, no causal relationship between changes in microseism and microtremor spectra were shown. However, as indicated in Figure 4a,b, there appears to be no clear relationship between the strength of the microtremor and the microseism signals.

### Array Analysis

Array analyses of double-frequency microseisms and microtremors have proven to be a powerful tool for isolating the coherent wave energy that composes the wave. Such analyses have provided detailed information not only on the phase velocity and direction of approach of the signals but also on the sources that are generating the wave field (Haubrich and McCamy, 1969; Satoh *et al.*, 2001; Chevrot *et al.*, 2007). In the study presented here the vertical component signals recorded from three-component broadband seismometers were selected and analyzed in 1 hr time windows. The data were first frequency band-pass filtered, followed by the application of a high-resolution wavenumber $(f_x - f_y)$ analysis technique (Capon, 1969) to determine the azimuths and the phase velocities (i.e., the velocity at which wavefronts sweep across the array). In each array the energy response was measured on a grid uniformly sampled in slowness and azimuth. This technique is used to identify the type of waves and the locations of the source of microseism and microtremor energies. The largest arrays deployed during the survey (with an aperture of 3600 m) were studied for characterization of the microseism signals.

Figure 5a,b,c represents the slowness maps for long-period and short-period double-frequency microseisms (Fig. 5a: location A, center frequency = 0.2 Hz; Fig. 5b: location B, center frequency = 0.2 Hz; Fig. 5c: location A, center frequency = 0.35 Hz). An arrow denotes the corresponding azimuth for the wavenumber vector at the peak spectrum amplitude. The signals in both bands show high coherency across the array and typically include a single well-defined peak that permits an estimation of phase velocities
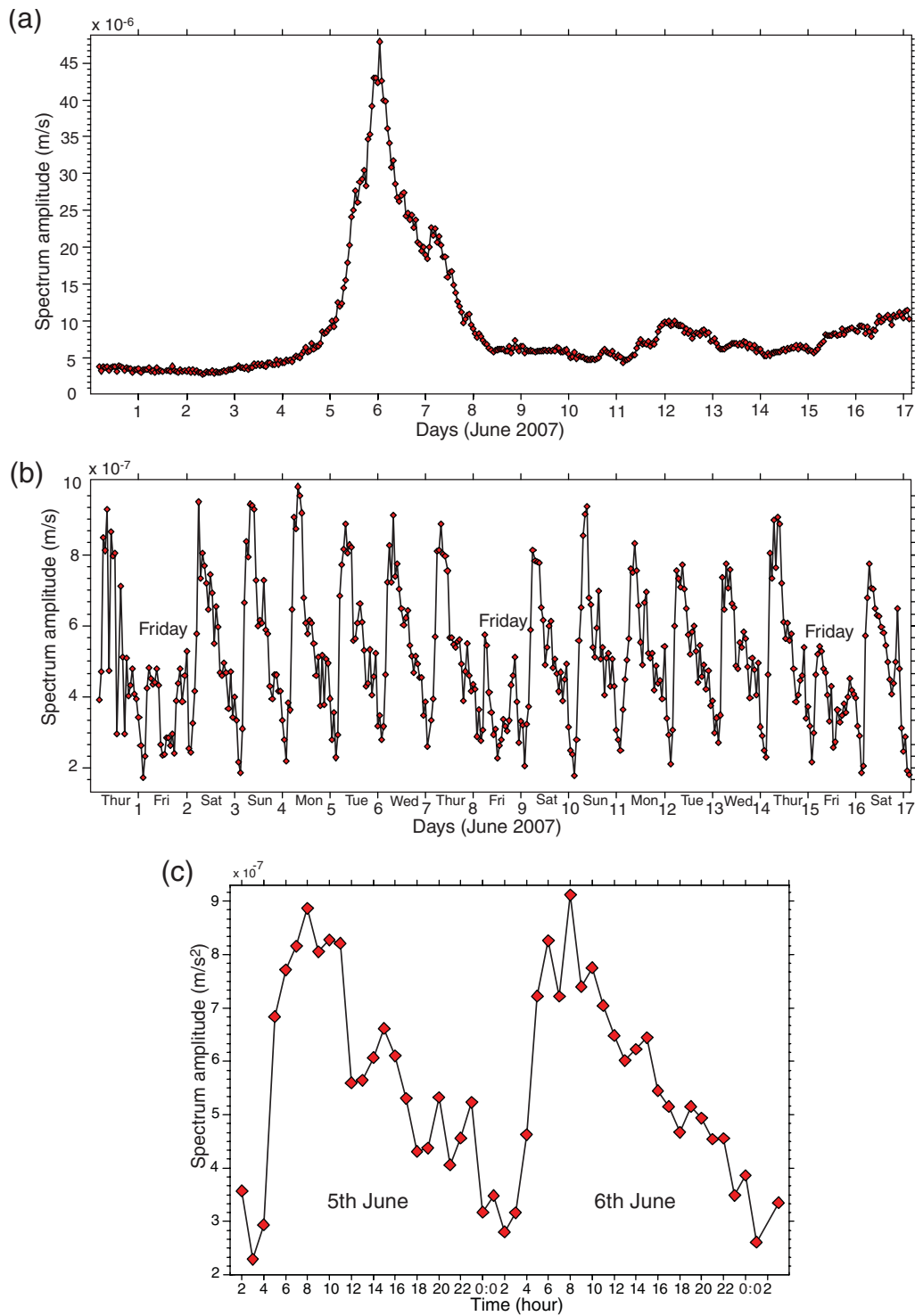
**Figure 4.**     (a) Peak spectral amplitudes of vertical component of double-frequency microseism (0.2 Hz) obtained at location B. (b) Peak spectral amplitudes of microtremor signal (2.5 Hz). (c) Peak spectral amplitudes of microtremor signal for 5 and 6 June 2007. The spectral amplitudes of microseisms increased dramatically when Cyclone Gonu approached the coast of Oman, whereas the microtremor signal remained unchanged. Spectral amplitudes of microtremor signals exhibit strong daily and weekly cyclical variations. Signals were significantly stronger during normal working hours on weekdays compared with night times and across weekends.

and propagation azimuth. The figure illustrates that the propagation azimuth (from the source) of the long-period double-frequency microseism wavefront varies from 305° to 327° with an apparent velocity of approximately 3600 m/sec corresponding to that of crustal Rayleigh waves (Bromirski, 2001). In both arrays the double-frequency microseism events are arriving from the southeast direction with slight variation of azimuth, probably due to a change in position of the source.
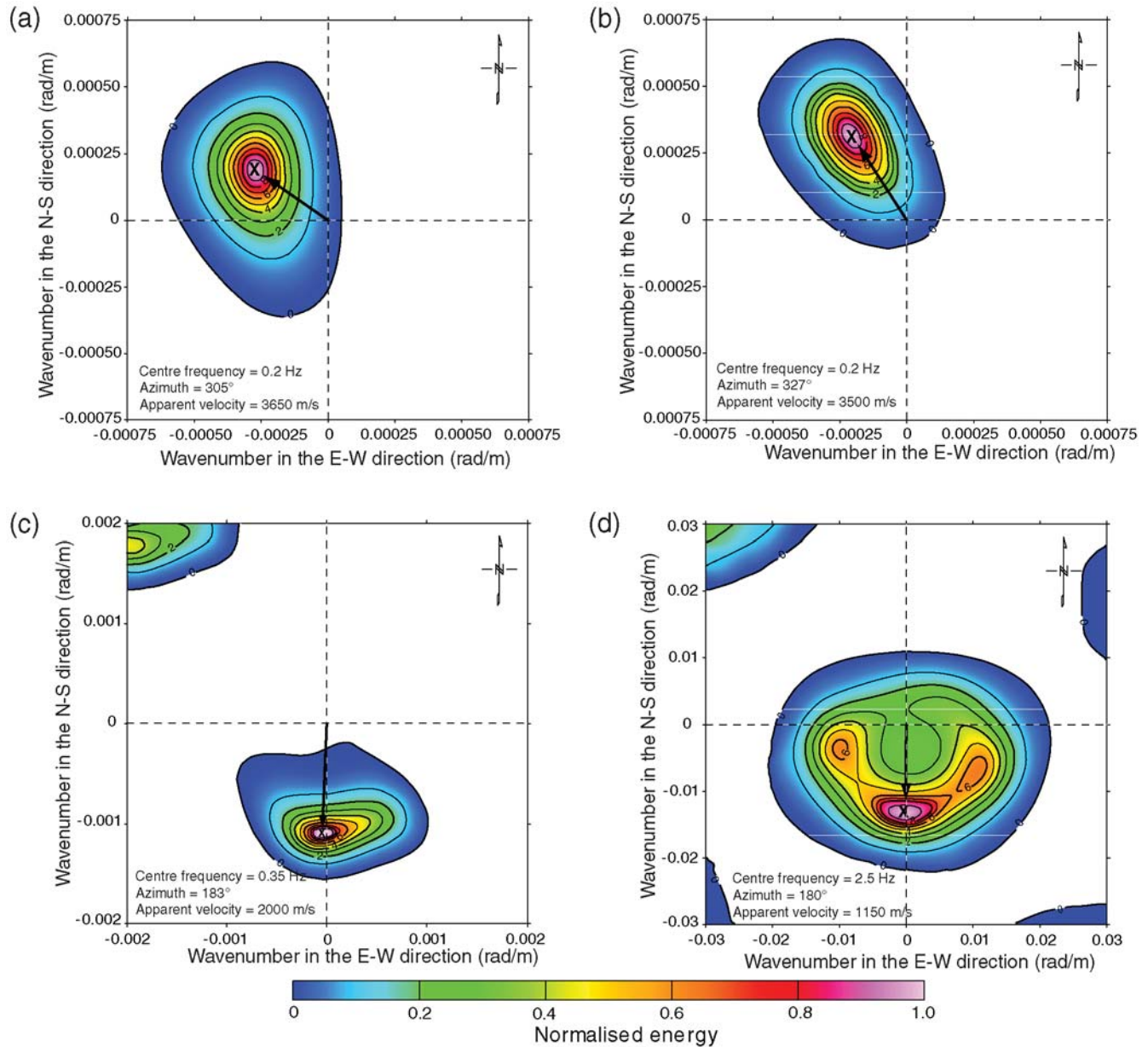
**Figure 5.** Normalized energy response in slowness space for arrays of varying aperture sizes at locations A and B. (a) Location A: center frequency, 0.2 Hz; array aperture, 3600 m; date and time, 4 June 2007 at 0:00–01:00. (b) Location B: center frequency, 0.2 Hz; array aperture, 3600 m; date and time, 16 June 2007 at 0:00–01:00. (c) Location A: center frequency, 0.35 Hz; array aperture, 3600 m; date and time, 4 June 2007 at 0:00–01:00. (d) Location A: center frequency, 2.5 Hz; array radius, 225 m; date and time, 26 May 2007 at 0:00–01:00. For locations of the sensors see Figure 1b. In each figure the symbol X indicates the peak values. The distance between the centers and X gives the slowness of the waves at the frequency, and the line at the center to X gives the direction of the wave propagation (apparent velocity equals $2\pi f/|k|$, and wavelength, $\lambda$, equals $2\pi|k|$, where $f$ is the frequency and $k$ is the wavenumber). The phase velocity and propagation azimuth (from the source) determined from the maximum peak are written in the lower left-hand corner in each plot.

Therefore, the wavefront is interpreted as a microseism event generated by wave activity in the Arabian Sea.

Examination of the phase velocities of the short-period double-frequency microseism (0.35 Hz) wavefront (Fig. 5c) indicates a tendency to cluster at approximately 2000 m/sec with a consistent propagation azimuth of 183°. The short-period double-frequency microseisms appear to be generated within local storms in the Arabian Gulf (40 km north of the

study area) due to the interaction between sea waves and the coast. Figure 5d shows the slowness map for the microtremor band (center frequency = 2.5 Hz) at location A with an aperture of 225 m. The propagation azimuth is relatively scattered although the maximum energy response is about 180° pointing in the direction of a major motorway. The apparent velocity of these wavefronts varies from 1150 to 1300 m/sec.

The study area is generally composed of a few meters of unconsolidated sand and sabkha, which directly overlie relatively hard carbonate layers with *P*-wave velocities that far exceed 1300 m/sec. Therefore, the observed wavefront cannot be an ordinary *P* wave that has originated from the subsurface hydrocarbon reservoir. If the recorded waves were coming from directly below the array then they would arrive simultaneously at all seismometers (i.e., the apparent velocity would be very high to infinite and the azimuth undefined). Thus, on the basis of these observations, the origin of the low-frequency microtremor noise may be attributed to surface-coupled waves excited by traffic loads predominantly coming from a major motorway 15–18 km north of the study area. This analysis is consistent with the interpretation drawn from the spectral amplitude analyses but is in apparent contrast with other studies that have attributed the spectral peaks of the microtremor events with the location of subsurface hydrocarbon reservoirs (Dangel *et al.*, 2003; Holzner *et al.*, 2005; Walker, 2008).

## Discussion and Conclusions

Cyclone Gonu generated large oceanic swells that coupled energy into the Earth in the form of seismic waves, detected in this study at distances greater than 500 km from the coastline. Such results are consistent with observations of microseisms in Southern California that were generated by Hurricane Katrina in New Orleans a distance of about 2700 km away (Gerstoft *et al.*, 2006).

Observations from the analyses of the spectral amplitudes and high-resolution wavenumber ($k_x - k_y$) studies have revealed that double-frequency microseism signals are clearly observed within the frequency band of 0.15–0.4 Hz. The spectral amplitudes of the microseism band exhibit a variation over time and correlate positively with the appearance of Cyclone Gonu that developed in the Arabian Sea during the survey.

Microtremor signals were consistently observed in the frequency band of 2–3 Hz. Spectral amplitudes of the microtremor signals showed daily and weekly cyclical variations, with minimums occurring from 01:00 to 03:00 and maximums around 08:00. Cultural activities were determined as the most probable cause of these variations, mainly due to the observed amplitude decrease during the night and across weekends. Furthermore, the analyses show no correlation between the microtremor and microseism signals, and therefore the driving force of the microtremor signal cannot be attributed to the microseism events.

Frequency–wavenumber analyses show a significant amount of coherent plane-wave propagation across the arrays in the microseisms and microtremor ranges. The apparent velocity and propagation azimuth (from the source) of long-period double-frequency microseism signal are 3600 m/sec and 305°–327° respectively for both locations A and B, respectively. These results suggest that the source of the long-period double-frequency microseism is the interaction of ocean swells of the Arabian Sea. The apparent velocity and propagation azimuth for the short-period double-frequency microseism signal recorded at location A are 2000 m/sec and 183°, respectively. These results indicate that the observed short-period double-frequency microseism signals originate from surface waves having an azimuth directed from the nearest coastline in the area (i.e., the Arabian Gulf).

The apparent velocity and propagation azimuth for the microtremor signal are 1150 m/sec and 180°, respectively. These results indicate that the observed microtremor signals originate from cultural activities having an azimuth toward the nearest motorway. Moreover, the fact that all three sensor components recorded the microtremor signal confirms that the signal cannot be a *P* wave traveling directly up from below the sensors (i.e., from the hydrocarbon reservoir). Rather the microtremor signal is interpreted as having originated from cultural sources (e.g., traffic and machine vibrations) propagating mainly as surface waves.

## Data and Resources

Data used in this study were acquired as a part of a project funded by the Oil-Subcommittee of the Abu Dhabi National Oil Company (ADNOC) and cannot be released to the public without prior approval. The location of the oil-water contact (OWC) of the oil field was provided by Abu Dhabi Company for Onshore Oil Operations (ADCO). Satellite images were obtained from http://earthobservatory.nasa.gov/NaturalHazards/view.php?id=18442 (last accessed August 2009).

Spectral and array analyses were made using the Geopsy software version 2.6.3 (www.geopsy.org, last accessed August 2009; Wathelet *et al.*, 2008). Some plots were made using the Geosoft Oasis Montaj version 7.0.1 (www.geosoft.com, last accessed August 2009).

## Acknowledgments

## References

Barstow, N., G. H. Sutton, and J. A. Carter (1989). Particle motion and pressure relationships of ocean bottom noise at 3900 m depth: 0.003 to 5 Hz, *Geophys. Res. Lett.* **16,** 1185–1188.

Bonnefoy-Claudet, S., F. Cotton, and P. Y. Bard (2006). The nature of noise wavefield and its applications for site effects studies—A literature review, *Earth Sci. Rev.* **79,** 205–227, doi 10.1016/j.earscirev.2006.07.004.

Bromirski, P. D. (2001). Vibrations from the "perfect storm", *Geochem. Geophys. Geosys.* **2,** no. 7, 1030, doi 10.1029/2000GC000119.

Bromirski, P. D., and F. K. Duennebier (2002). The near-coastal microseism spectrum: Spatial and temporal wave climate relationships, *J. Geophys. Res.* **107,** no. B8, 2166, doi 10.1029/2001JB000265.

Bromirski, P. D., F. K. Duennebier, and R. A. Stephen (2005). Mid-ocean microseisms, *Geochem. Geophys. Geosys.* **6,** Q04009, doi 10.1029/2004GC000768.

Capon, J. (1969). High-resolution frequency-wavenumber spectrum analysis, *Proc. IEEE* **57,** 1408–1418.

Chevrot, S., M. Sylvander, S. Benahmed, C. Ponsolles, J. M. Lefevre, and D. Paradis (2007). Source locations of secondary microseisms in western Europe: Evidence for both coastal and pelagic sources, *J. Geophys. Res.* **112,** B11301, doi 10.1029/2007JB005059.

Dangel, S., M. E. Schaepman, E. P. Stoll, R. Carniel, O. Barzandji, E. D. Rode, and J. M. Singer (2003). Phenomenology of tremor-like signals observed over hydrocarbon reservoirs, *J. Volcanol. Geotherm. Res.* **128,** 135–158.

Gerstoft, P., and T. Tanimoto (2007). A year of microseisms in Southern California, *Geophys. Res. Lett.* **34,** L20304, doi 10.1029/2007gl031091.

Gerstoft, P., M. C. Fehler, and K. G. Sabra (2006). When Katrina hit California, *Geophys. Res. Lett.* **33,** L17308, doi 10.1029/2006GL027270.

Hanssen, P., and S. Bussat (2008) Pitfalls in the analysis of low frequency passive seismic data, *First Break* **26,** 111–119.

Haubrich, R. A., and K. McCamy (1969). Microseisms; Coastal and pelagic sources, *Rev. Geophys.* **7,** no. 3, 539–571.

Holzner, R., P. Eschle, S. Dangel, M. Frehner, C. Narayanan, and D. Lakehal (2009). Hydrocarbon microtremors interpreted as nonlinear oscillations driven by oceanic background waves, *Commun. Nonlinear Sci. Numer. Sim.* **14,** 160–173.

Holzner, R., P. Eschle, H. Zurcher, M. Lambert, R. Graf, S. Dangel, and P. F. Meier (2005). Applying microtremor analysis to identify hydrocarbon reservoirs, *First Break* **23,** 41–46.

Kedar, S., and F. H. Webb (2005). The ocean's seismic hum, *Science* **307,** 682–683, doi 10.1126/science.1108380.

Konno, K., and T. Ohmachi (1998). Ground-motion characteristics estimated from spectral ratio between horizontal and vertical components of microtremor, *Bull. Seismol. Soc. Am.* **88,** 228–241.

Lambert, M.-A., S. M. Schmalholz, E. H. Saenger, and B. Steiner (2009). Low-frequency microtremor anomalies at an oil and gas field in Voitsdorf, Austria, *Geophys. Prospect.* **57,** 393–411, doi 10.1111/j.1365-2478.2008.00734.x.

le Comte, D. (2008). Global weather highlights 2007: A mixed bag, *Weatherwise* **61,** 16–18.

Longuet-Higgins, M. S. (1950). A theory of the origin of microseisms, *Phil. Trans. R. Soc. London A* **243,** 1–35, doi 10.1098/rsta.1950.0012.

Marzorati, S., and D. Bindi (2006). Ambient noise levels in north central Italy, *Geochem. Geophys. Geosys.* **7,** Q09010, doi 10.1029/2006GC001256.

McNamara, D. E., and R. P. Buland (2004). Ambient noise levels in the continental United States, *Bull. Seismol. Soc. Am.* **94,** no. 4, 1517–1527.

Oliver, J., and M. Ewing (1957). Microseisms in the 11- to 18-second period range, *Bull. Seismol. Soc. Am.* **47,** 111–127.

Peterson, J. (1993). Observations and modeling of seismic background noise, *U.S. Geol. Surv. Open-File Rept. 93-322*, 1–95.

Saenger, E. H., S. M. Schmalholz, M. A. Lambert, T. T. Nguyen, A. Torres, S. Metzger, R. M. Habiger, T. Muller, S. Rentsch, and E. Mendez-Hernandez (2009). A passive seismic survey over a gas field: Analysis of low-frequency anomalies, *Geophysics* **74,** O29–O40, doi 10.1190/1.3078402.

Satoh, T., H. Kawase, and S. Matsushima (2001). Estimation of *S*-wave velocity structures in and around the Sendai basin, Japan, using array records of microtremors, *Bull. Seismol. Soc. Am.* **91,** 206–218.

Steiner, B., E. H. Saenger, and S. M. Schmalholz (2008). Time reverse modeling of low-frequency microtremors: Application to hydrocarbon reservoir localization, *Geophys. Res. Lett.* **35,** L03307, doi 10.1029/2007GL032097.

Tanimoto, T. (2007). Excitation of normal modes by non-linear interaction of ocean waves, *Geophys. J. Int.* **168,** 571–582, doi 10.1111/j.1365-246X.2006.03240.x.

Walker, D. (2008). Recent developments in low frequency spectral analysis of passive seismic data, *First Break* **26,** 69–77.

Wathelet, M., D. Jongmans, M. Ohrnberger, and S. Bonnefoy-Claudet (2008). Array performances for ambient vibrations on a shallow structure and consequences over $V_S$ inversion, *J. Seism.* **12,** 1–19.

Webb, S. C. (2007). The Earth's "hum" is driven by ocean waves over the continental shelves, *Nature* **445,** 754–756, doi 10.1038/nature05536.

Withers, M. M., R. C. Aster, C. J. Young, and E. P. Chael (1996). High-frequency analysis of seismic background noise as a function of wind speed and shallow depth, *Bull. Seismol. Soc. Am.* **86,** no. 5, 1507–1515.

Yamanaka, H., M. Dravinski, and H. Kagami (1993). Continuous measurements of microtremors on sediments and basement in Los Angeles, California, *Bull. Seismol. Soc. Am.* **83,** 1595–1609.

The Petroleum Institute
P.O. Box 2533
Abu Dhabi, United Arab Emirates
mali@pi.ac.ae